comparable statistics using this measure would require long-term residence by several fieldworkers in many separate villages (*24*).

36. In each of the four age categories, the *unokais* were characterized by both more children and more wives than non-*unokais*. For Table 2, all age categories yielded chi-square values statistically significant at at least the 0.05 level. For Table 3 the chi-square values were not statistically significant for age categories 25 to 30 and 31 to 40 but were at the 0.05 level for the other two age categories. For both Tables 2 and 3, the pooled data (totals) were significant ($P < 0.00001$). In both tables the differences between expected and observed values were in the same direction for all age categories and pooled.
37. R. Spielman, thesis, University of Michigan, Ann Arbor (1971); R. Spielman *et al.*, *Am. J. Phys. Anthropol.* **37**, 345 (1972); R. Spielman, *Am. Nat.* **107**, 694 (1973). During the anthropometric field studies the biomedical personnel, unfamiliar with the life histories of the individuals, informally attempted to guess whether or not particular men being measured were among the *waiteri* (fierce ones), were political leaders, or were otherwise prominent in the group; comparison of their predictions against my life history data on these same individuals showed uniformly poor results.
38. Many U.S. congressmen are and traditionally have been reserve officers in the U.S. Army [E. Hoebel, in *War: The Anthropology of Armed Conflict and Aggression*, M. Fried, R. Murphy, M. Harris, Eds. (Natural History Press, Garden City, NY, 1968), pp. 208–210].
39. L. Betzig, *Despotism and Differential Reproduction: A Darwinian View of History* (Aldine, New York, 1986).
40. C. Levi-Strauss, in an article on "chieftainship" in a South American tribal society, the Nambikwara of Brazil [*Trans. N.Y. Acad. Sci.* **7**, 16 (1944)], argued that tribal communities might profitably be viewed as clusters of people who form around prominent men whose only compensation for the onerous tasks of leadership was the concession the group made to the leaders in the form of multiple wives.
41. Ironically, this man was married polyandrously. His duties as a practical nurse did not allow him time to garden so he had to compromise and share his wife with another man who had a garden.
42. Field research was sponsored by NSF and the Harry Frank Guggenheim Foundation and data analysis by the Harry Frank Guggenheim Foundation. I would like to thank R. Alexander, R. Axelrod, D. Brown, R. Carneiro, R. Hames, M. Daly, T. Harding, M. Harrell, W. Irons, M. Meggitt, S. Plattner, D. Symons, R. Thornhill, and P. Van den Berghe, for critical comments on this manuscript. I thank M. de la Luz Ibarra and E. Kargard for assistance with library research, manuscript preparation, graphics, and computer analyses. I thank A. Spaulding for assistance on the statistical tests.

Quantum Mechanics of a Macroscopic Variable: The Phase Difference of a Josephson Junction

JOHN CLARKE, ANDREW N. CLELAND, MICHEL H. DEVORET, DANIEL ESTEVE, JOHN M. MARTINIS

Experiments to investigate the quantum behavior of a macroscopic degree of freedom, namely the phase difference across a Josephson tunnel junction, are described. The experiments involve measurements of the escape rate of the junction from its zero voltage state. Low temperature measurements of the escape rate for junctions that are either nearly undamped or moderately damped agree very closely with predictions for macroscopic quantum tunneling, with no adjustable parameters. Microwave spectroscopy reveals quantized energy levels in the potential well of the junction in excellent agreement with quantum-mechanical calculations. The system can be regarded as a "macroscopic nucleus with wires."

ARE MACROSCOPIC DEGREES OF FREEDOM GOVERNED BY quantum mechanics? Our everyday experience tells us that a classical description appears to be entirely adequate. The trajectory of the center of mass of a billiard ball is predicted wonderfully well by classical mechanics. Even the Brownian motion of a tiny speck of dust in a drop of water is a purely classical phenomenon. Until recently, quantum mechanics manifested itself at the macroscopic level only through such collective phenomena as superconductivity, flux quantization, or the Josephson effect. However, these "macroscopic" effects actually arise from the coherent superposition of a large number of microscopic variables each governed by quantum mechanics. Thus, for example, the current through a Josephson tunnel junction and the phase difference across it are normally treated as classical variables. As Leggett (*1*) has emphasized, one must distinguish carefully between macroscopic quantum phenomena originating in the superposition of a large number of microscopic variables and those displayed by a single macroscopic degree of freedom. It is the latter that we discuss in this article.

Our usual observations on a billiard ball or Brownian particle reveal classical behavior because Planck's constant $\hbar$ is so tiny. However, at least in principle there is nothing to prevent us from designing an experiment in which these objects are quantum mechanical. To do so we have to satisfy two criteria: (i) the thermal energy must be small compared with the separation of the quantized energy levels, and (ii) the macroscopic degree of freedom must be sufficiently decoupled from all other degrees of freedom if the lifetime of the quantum states is to be longer than the characteristic time scale of the system (*1*). To illustrate the application of these criteria, following Leggett (*1*) we consider a simple harmonic oscillator consisting of an inductor L connected in parallel with a capacitor C. The flux Φ in the inductor and charge q on the capacitor are macroscopic conjugate variables. Observations on the oscillator are made by means of leads that unavoidably couple it to the environment. The dissipation so introduced is represented by a resistor R in parallel with L and C. The natural angular frequency of oscillation is $\omega_0 = (LC)^{-1/2}$, the impedance at the resonance frequency is $Z_0 = (L/C)^{1/2}$, and the quality factor (ratio of stored energy to energy dissipated in one oscillation) is $Q = \omega_0 CR = R/Z_0$. To observe quantum effects we thus require (i) $\hbar\omega_0 >> k_B T$, where

J. Clarke and A. N. Cleland are in the Department of Physics, University of California, and the Materials and Chemical Sciences Division, Lawrence Berkeley Laboratory, Berkeley, CA 94720. During the time these experiments were performed M. H. Devoret and J. M. Martinis were at the same address; they and D. Esteve are currently at Service de Physique, Centre d'Études Nucléaires de Saclay, 91191 Gif-sur-Yvette Cedex, France.

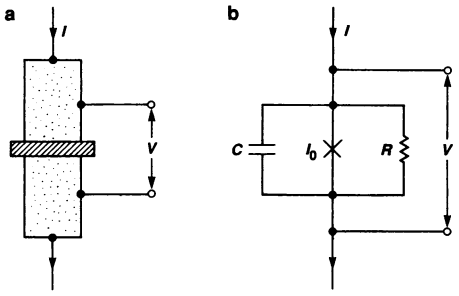

Fig. 1. (**a**) Schematic representation and (**b**) circuit description of Josephson tunnel junction.

T is the temperature of the system, and (ii) $R >> Z_0$. To give a numerical example, we assume that we are willing to cool our system to 10 mK, and that the leads coupled to the junction have a characteristic impedance Z_c of 50 ohms. To ensure the oscillator is comfortably in the quantum limit we impose the constraints $\omega_0 > 10k_BT/\hbar$ and $Z_c > 10\ Z_0$, and find $\omega_0/2\pi > 2$ GHz, $L < 350$ pH, and $C < 15$ pF. Thus, for this system one can hope to challenge the smallness of $\hbar$.

Even though we have been rather conservative in our constraints, we see that the required components are "off the shelf." Thus, it seems straightforward to construct a macroscopic oscillator exhibiting quantum behavior. Unfortunately, it is not nearly so straightforward to demonstrate that the oscillator is behaving quantum mechanically. For example, transitions between adjacent energy levels would always involve quanta of frequency ω_0, which is of course precisely the frequency one observes classically: the simple harmonic oscillator is in the correspondence limit (*2*) for all quantum numbers. Alternatively, one could attempt to observe the zero-point motion of the ground state, a clear signature of quantum behavior. This is, however, an extremely difficult experiment requiring a quantum-limited amplifier.

Fortunately, one can "evade the correspondence limit" by using a Josephson tunnel junction (*3*). The macroscopic degree of freedom is the difference δ between the phases of the condensates of Cooper pairs in the superconductors on either side of the tunnel barrier. As we shall see later, in the classical limit the junction behaves as a nonlinear inductor shunted by a capacitor. The anharmonicity of the oscillator resulting from the nonlinearity has two important consequences enabling us to observe the quantum behavior of a macroscopic variable. First, one can demonstrate the existence of a wave packet associated with δ by observing the decay of the ground state by "macroscopic quantum tunneling." Second, the separation of adjacent energy levels decreases with increasing quantum number so that one can demonstrate energy quantization spectroscopically.

Dynamics of a Josephson Junction

A Josephson tunnel junction (Fig. 1a) consists of two superconductors separated by a thin insulating barrier (*3*). Cooper pairs, that is, electrons of equal and opposite momenta and having paired spins, can tunnel through the barrier with no voltage drop; this flow of pairs constitutes a supercurrent. One can pass a static supercurrent through the junction up to a maximum value I_0, known as the critical current. The junction (Fig. 1b) has a self-capacitance C and is shunted by a resistance R that often arises from external circuitry, as we shall see later. When the external current I is increased from zero the phase difference across the junction is given by the Josephson current-phase relation $I = I_0 \sin\delta$; when I exceeds I_0, a voltage is developed across the junction and δ evolves with time according to the Josephson voltage-frequency relation $\dot{\delta} = 2\pi V/\Phi_0$, where $\Phi_0 = h/2e$ is the flux quantum. If we set the sum of the current flowing through the three elements of the junction in Fig. 1b equal to I and eliminate terms in V in favor of δ, we arrive at the following classical equation of motion for the phase difference:

$$C\left(\frac{\Phi_0}{2\pi}\right)^2 \ddot{\delta} + \frac{1}{R}\left(\frac{\Phi_0}{2\pi}\right)^2 \dot{\delta} + \frac{\partial U(\delta)}{\partial \delta} = \frac{\Phi_0}{2\pi} I_N(t) \qquad (1)$$

The term $I_N(t)$ represents the Nyquist current noise generated by the resistor R at temperature T, and (*3*)

$$U(\delta) = -(I_0\Phi_0/2\pi)[\cos\delta + (I/I_0)\delta] \qquad (2)$$

One achieves great insight into the dynamics of the junction by realizing that Eq. 1 is identical to the classical equation of motion of the coordinate δ of a particle with mass $C(\Phi_0/2\pi)^2$ moving in the tilted washboard potential $U(\delta)$ shown in Fig. 2. The average slope of the washboard is proportional to $-I/I_0$. For $I < I_0$ the potential has relative minima, and the particle can be trapped in one of them (Fig. 2a). However, although the average value $\langle\dot{\delta}\rangle$ and hence the time-averaged voltage V across the junction are zero in this state, it is important to realize that the particle is not stationary, but rather that it oscillates at the bottom of the well at the so-called plasma frequency (*3*)

$$\omega_p = (2\pi I_0/\Phi_0 C)^{1/2}[1 - (I/I_0)^2]^{1/4} \qquad (3)$$

If we increase the bias current, eventually the particle will escape from the well and propagate down the washboard (Fig. 2b); in this state both δ and V are nonzero.

The exact correspondence between the motion of the particle and the dynamics of δ is very useful, since it provides a heuristic model with which one can understand the dynamics of the junction. As it is more straightforward to discuss the behavior of this fictitious particle than the motion of δ, we shall do so freely in the remainder of this article, which is concerned with the processes by which the particle escapes from the well (that is, the junction makes a transition from the zero-voltage state to the nonzero-voltage state). To aid this discussion, in Fig. 2, c and d, we show a single potential well. In the experiments to be described I is very close to I_0 and the potential is of the form $A\delta^2 - B\delta^3$ ($A, B > 0$). In this approximation the barrier height is (*4*)

$$\Delta U = [2(2)^{1/2} I_0\Phi_0/3\pi](1 - I/I_0)^{3/2} \qquad (4)$$

The damping of the oscillations by the resistance R (assumed to be linear) is represented by

$$Q = \omega_p RC \qquad (5)$$

In this classical description, the particle can escape from the well as a result of thermal activation: the fluctuating thermal energy of the particle eventually exceeds ΔU and the particle escapes over the top of the barrier. The escape rate for thermal activation is given by the Kramers' result (*5*)

$$\Gamma_t(T) = a_t(\omega_p/2\pi)\exp(-\Delta U/k_BT) \qquad (6)$$

where the prefactor a_t is of order unity (*6*). The thermal energy of the particle arises from the noise current $I_N(t)$.

In thermal activation, the system is entirely classical and is described by a classical equation of motion representing a point particle with a continuous range of energy (Fig. 2c). The phase difference δ is a classical variable. If we lower the temperature, Eq. 1 is no longer valid since the dynamics of the particle must be described quantum mechanically. The crossover from the classical to the quantum mechanical description occurs at a temperature (*7*) $T_{cr} = \hbar\omega_p/2\pi k_B$ (for $Q >> 1$). Below this temperature, the phase difference δ must be represented by a quantum mechanical operator, rather than treated as a classical variable. The position of the particle is now described by a wave packet, $\psi(\delta)$, and the energy of the

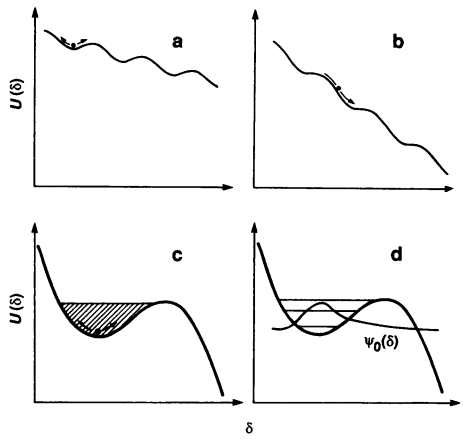

Fig. 2. Tilted washboard analog of Josephson tunnel junction: (**a**) stationary state ($V = 0$) for $I < I_0$, and (**b**) running state ($V \neq 0$) for $I > I_0$. In the stationary state in the classical regime (**c**) the particle is point-like with a continuous energy range, whereas in (**d**) the ground state $\psi_0(\delta)$ of the particle is described by a wave packet and the energy is quantized into levels.

particle can assume only discrete values corresponding to eigenstates of the system (Fig. 2d). The leakage of $\psi(\delta)$ under the barrier enables the particle to escape from the well by macroscopic quantum tunneling (MQT) through the barrier (*1, 8, 9*).

We now emphasize the distinction between Josephson tunneling and macroscopic quantum tunneling. In Josephson tunneling the passage of each Cooper pair is controlled by the difference δ in the phase of the pair across the barrier. Since the condensate in any piece of superconductor is characterized by a single phase, the phase difference δ for all pairs must be the same. Thus, δ is "macroscopic" in the sense that it is the single variable that completely specifies the state of the junction, that is, of all the Cooper pairs. In the process of macroscopic quantum tunneling it is the particle associated with the phase difference δ that tunnels as opposed to the tunneling of individual Cooper pairs that occurs in Josephson tunneling. Thus, the demonstration that MQT takes place implies that δ is a quantum variable, that is, that one must represent it by a wave packet. By contrast, although δ represents the phase difference between two macroscopic quantum states, in the majority of experiments on Josephson tunneling it is nonetheless a classical variable, describable by purely classical equations.

The first calculation of the tunneling rate was made by Ivanchenko and Zil'berman (*8*) for a junction at $T = 0$ with no dissipation. A major step forward was made by Caldeira and Leggett (*9*) who calculated the reduction in the tunneling rate when a linear damping resistor was connected across the junction. To first order in $1/Q$ at $T = 0$ they predicted the escape rate to be

$$\Gamma_q(0) = \left[120\pi\left(\frac{7.2\Delta U}{\hbar\omega_p}\right)\right]^{1/2} \frac{\omega_p}{2\pi} \exp\left[-7.2\frac{\Delta U}{\hbar\omega_p}\left(1 + \frac{0.87}{Q}\right)\right] \quad (7)$$

The reduction of $\Gamma_q(0)$ by dissipation arises from a narrowing of the wave packet. In the limit $Q \to \infty$, $\Gamma_q(0)$ reduces to the Wentzel-Kramer-Brillouin (WKB) result (*2*) obtained by Ivanchenko and Zil'berman (*8*). Subsequently, many other theoretical papers have appeared; the reviews listed in (*10*) give a comprehensive summary. The theory has been extended to nonzero temperatures (*7, 11–16*): when $T \sim T_{cr}$, both MQT and thermal activation contribute to the escape process. There is also a large body of literature (*10*) concerned with a related system, namely, a superconducting loop interrupted by a single Josephson junction, which exhibits similar behavior to that described above.

Detailed measurements of thermal escape in the classical regime $T >> T_{cr}$ were made by Jackel *et al.* (*17*) and Fulton and Dunkleberger (*4*) on a junction in a superconducting loop and on a current-biased junction, respectively. The first attempts to measure MQT were made by Ouboter and co-workers (*18*), Voss and Webb (*19*), and Jackel *et al.* (*20*). The results of these experiments and of several others (*21–23*) agreed qualitatively with theory in that the escape rate tended to become constant as the temperature was lowered and tended to be reduced as the dissipation was increased. In these experiments, a persistent difficulty has been the lack of knowledge of the junction parameters in the relevant microwave frequency range. However, Schwartz *et al.* (*24*) performed experiments on a loop containing a junction shunted with an external resistor and made separate measurements of the relevant parameters. In the overdamped limit ($Q << 1$) of their experiment, a recent reanalysis of their results shows them to be in quite good agreement with theory (*25*).

In the present work, we used classical phenomena to measure the parameters I_0, C, and R in situ, so that we are able to compare experiment and theory in the quantum regime with no adjustable parameters (*26*). A further important consideration is the elimination of spurious noise from the junction. We address both issues in the next two sections.

Experimental Details

We deposited tunnel junctions on 10 by 10 mm^2 oxidized silicon chips using standard photolithographic processing. The base electrode consisted of a niobium film typically 10 μm wide and 0.2 μm thick; after oxidizing the film we deposited a PbIn counterelectrode at right angles to it. The junction was attached to a mount in thermal contact with the mixing chamber of a dilution refrigerator capable of reaching about 20 mK (Fig. 3).

A series of low-pass filters eliminated thermal noise from the measuring apparatus and spurious signals such as those from radio stations, while allowing us to interrogate the junction at low frequencies. These filters were of two kinds: radio-frequency filters consisting of resistors or inductors and capacitors, and custom-made microwave filters. The microwave filters consisted of a spiral of insulated wire inside a copper tube filled with copper powder with a grain size of about 30 μm. Since each grain is insulated from its

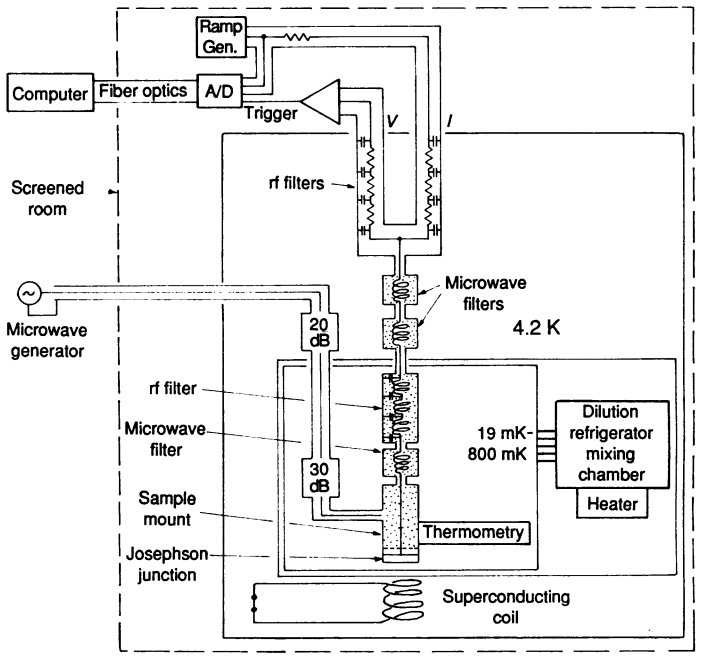

Fig. 3. Schematic drawing of apparatus.

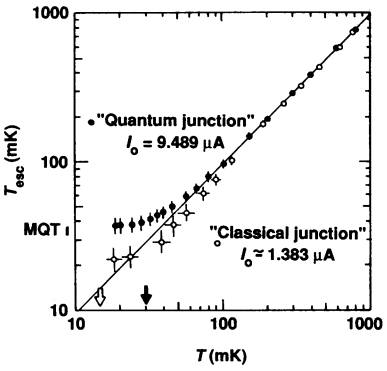

Fig. 4. T_{esc} versus T at $\ell n(\omega_p/2\pi\Gamma) = 11$ for the high and low values of I_0 with arrows indicating T_{cr} (solid and open circles and arrows). The vertical bar labeled MQT is the prediction for $I_0 = 9.489$ μA. The line is the thermal prediction $T_{esc} = 0.95T$. Horizontal error bars are a combination of systematic and random errors in the temperature scale; vertical error bars indicate primarily systematic uncertainties in the junction parameters. For clarity, error bars for T have been shown for the "classical junction" only; identical errors apply to the "quantum junction."

neighbors by an oxide layer, the effective surface area of the copper is enormous, producing substantial skin effect losses. The chain of filters provided an overall attenuation of more than 200 dB over the frequency range from 0.1 to 12 GHz. The last stage of filtering was engineered with particular care since it imposed the damping of the junction and hence determined Q. The junction was mounted as close as possible to the end of the filter to ensure that the impedance discontinuity between the junction and the line occurred in a distance small compared with the wavelength at the plasma frequency. Thus, the impedance attached to the junction behaved approximately as a parallel combination of a resistor and a capacitor.

To ascertain the escape rate Γ we applied a current ramp (Fig. 3) to the junction, and measured the value of current at which the appearance of a voltage signified the escape of the particle from the well. This value was digitized and transmitted to a computer outside the screened room surrounding the refrigerator by an optical fiber link. This measurement was repeated a large number of times, typically 10^5. Since the escape process is stochastic, one obtains a histogram representing the escape probability versus bias current. From this distribution it is straightforward (*4*) to derive the escape rate as a function of current, $\Gamma(I)$.

Determination of Junction Parameters in the Classical Regime

We now discuss the measurement of the parameters I_0, C, and R in the classical regime. We determined the parameters ω_p and Q using a technique based on a phenomenon we called resonant activation (*27*). The phenomenon is of interest in its own right in that it describes the escape of a Brownian particle from a potential well under the influence of a weak, sinusoidal force. Resonant activation involves the enhancement of the escape rate by a microwave current applied to the junction. When the microwave frequency is in the vicinity of ω_p, the particle is raised to a state of higher energy, and its probability of activation over the barrier is increased. The enhancement in the escape rate is manifested as an asymmetric peak that falls relatively rapidly on the high frequency side and has a long tail on the low frequency side. The asymmetry is a consequence of the anharmonicity of the potential well. With the aid of numerical simulations (*27*), we can determine $\omega_p(I)$ and $Q(I)$ from this resonance.

To determine I_0 we measured $\Gamma(0)$ in the classical regime in the absence of microwaves. As is evident from Eqs. 4 and 6 a plot of the experimentally determined quantity $\{\ell n[\omega_p(I)/2\pi\Gamma(I)]\}^{2/3}$ versus I should yield a straight line with slope scaling as $T^{-2/3}$ that intersects the current axis very close to I_0. After correcting for the departure of a_t from unity (*6*) and for the approximation made in Eq. 4, we find that the values of I_0 obtained in the temperature range 50 to 800 mK are in very good agreement. We also find good agreement between the temperatures inferred from the slope of the data and our thermometers.

Given I_0 and $\omega_p(I)$ we can infer C using Eq. 3 and hence R from Eq. 5. The values of I_0, C, and R, determined from purely classical experiments, are summarized in Table 1. The error in I_0 is the standard deviation arising from statistical uncertainties. The quoted errors in C and R, which arise from the fact that these quantities vary with bias current and thus with frequency, are a measure of the departure of the junction and its leads from the simple lumped-circuit model shown in Fig. 1. The fractional error in C is small because the self-capacitance of the junction was chosen to be as large as possible to minimize the effects of the leads. The fractional error in R is large, but in this particular experiment we wished to demonstrate only that Q was large enough for the effect of dissipation on Γ_q to be negligible. We note that the measured value of R is at least one order of magnitude less than the junction resistance determined at low voltages from the static I-V characteristic, indicating that the dissipation is almost completely determined by the bias circuitry.

Macroscopic Quantum Tunneling

We have found it convenient to express our escape rates in both classical and quantum regimes in terms of an escape temperature T_{esc} defined through the relation

$$\Gamma = (\omega_p/2\pi)\exp(-\Delta U/k_B T_{esc}) \quad (8)$$

In the classical regime T_{esc} is very nearly equal to T with a small correction due to the departure of a_t from unity. In the quantum regime T_{esc} takes a temperature-independent value that can be calculated exactly by comparing Eqs. 7 and 8. All of the parameters entering T_{esc} are measured experimentally.

We have made extensive measurements of $\Gamma(T)$ as a function of bias current over the temperature range from 19 to 800 mK. The derived values of T_{esc} are plotted versus T in Fig. 4. Above about 100 mK, T_{esc} follows the thermal prediction rather accurately. At lower temperatures T_{esc} flattens off to a temperature-independent value of 37.4 ± 4 mK, which is in good agreement with the Caldeira-Leggett $T = 0$ prediction of 36.0 ± 1.4 mK, with no adjustable parameters. The error in the experimental value is due primarily to the uncertainty in I_0; the error in the predicted value is due primarily to the uncertainty in C. The errors include possible systematic errors in the estimates of I_0 and C, respectively. These values of T_{esc} imply that the measured value of $\Gamma(0)$ is within a factor of 2 of the predicted value. We note that the contribution of the damping to the predicted value of T_{esc} is −1.5 mK, so that given

Table 1. Measured parameters for a shunted and unshunted Josephson tunnel junction, with experimental (T^e_{esc}) and predicted (T^p_{esc}) escape temperatures at $T = 0$ extrapolated from results at higher temperatures. The predicted values of T^p_{esc} for $Q = \infty$ are also included for comparison.

Quantity	Unshunted junction	Shunted junction
I_o (μA)	9.489 ± 0.007	24.873 ± 0.004
C (pF)	6.35 ± 0.4	4.28 ± 0.34
R (ohms)	190 ± 100	9.3 ± 0.1
Q	30 ± 15	1.77 ± 0.07
T^e_{esc} (mK)	37.4 ± 4.0	44.4 ± 1.7
T^p_{esc} (mK)	36.0 ± 1.4	42.5 ± 2.1
T^p_{esc} ($Q = \infty$)	37.5 ± 1.4	69 ± 3

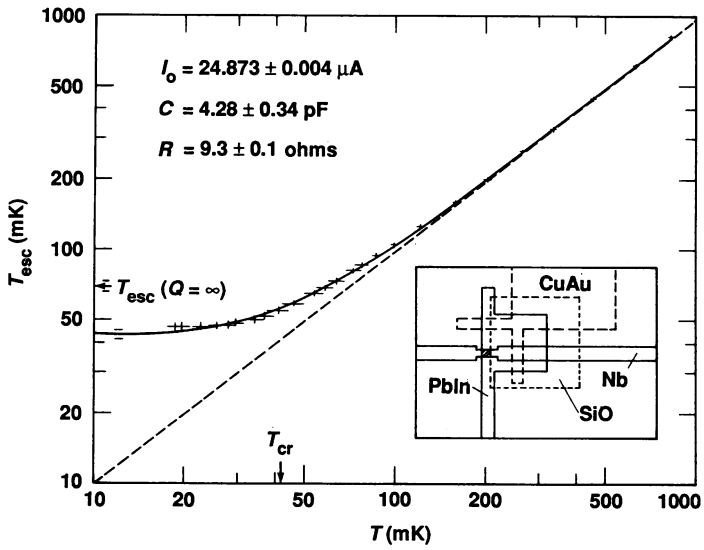

Fig. 5. T_{esc} versus T for shunted junction (configuration shown in inset). Solid curve is theory, dashed line is classical prediction $T_{esc} = 0.98T$. The crossover temperature T_{cr} for this junction and T_{esc} for $Q = \infty$ are indicated by arrows. Error bars are as in Fig. 4.

the combined experimental and theoretical uncertainties the effect of dissipation on $\Gamma_q(0)$ is negligible.

Although the measured low-temperature values of T_{esc} are in good agreement with predictions, nonetheless one should demonstrate that the flattening of T_{esc} as T is lowered is not due to an unknown, spurious noise source. In other words, we wish to show that the temperature "seen" by the junction is not significantly higher than that recorded by our thermometers. We carried out a self-check by applying a magnetic field (Fig. 3) to reduce I_0 and hence ω_p (see Eq. 3), thereby lowering T_{cr} to about 15 mK. The measured values of T_{esc} are close to the classical prediction, indicating that the flattening of T_{esc} for the higher value of critical current did not arise from spurious noise sources.

Thus, we have demonstrated the correctness of the prediction for $\Gamma_q(0)$ (Eq. 7) for the undamped case. To investigate the effects of dissipation on $\Gamma_q(0)$, we fabricated a series of junctions with a metallic shunt (*28*) deposited directly on the chip (inset, Fig. 5). The shunt was connected to a 1-mm^2 cooling fin to reduce the effects of heating after the junction switched to the $V \neq 0$ regime. After depositing and patterning the CuAu and Nb films we deposited an insulating layer of SiO. We then oxidized the Nb film and deposited a PbIn counterelectrode that also provided a superconducting groundplane to reduce the self-inductance of the shunt to a negligible level. The resistance of the shunt was determined from the measured current-voltage characteristics, and is therefore known to relatively high accuracy; C and I_0 were determined as described earlier.

The measured values of T_{esc} for one such junction are plotted versus T in Fig. 5. The solid line showing the predictions of the theory with no adjustable parameters is in good agreement over the entire temperature range. In particular, T_{esc} has been reduced substantially from the value expected for the same parameters with $Q = \infty$ (see Fig. 5 and Table 1). If one expresses the results in terms of escape rates, at a particular bias current of 24.71 μA the measured value of $\Gamma(0)$ is $1.2^{+0.7}_{-0.4} \times 10^4$ sec^{-1} compared with a predicted value of $0.62^{+0.58}_{-0.31} \times 10^4$ sec^{-1}; the experimental uncertainty is due to counting statistics, whereas the theoretical uncertainty comes from systematic uncertainties in the junction parameters. This rate is more than two orders of magnitude lower than that predicted for a junction with the same parameters but no damping, $(1.9 \pm 0.9) \times 10^6$ sec^{-1}. Thus, the observed tunneling rate has been greatly reduced by dissipation to a value in excellent agreement with theory.

For $0 < T < T_{cr}$, theory (*12*) predicts that $\ell n[\Gamma(T)/\Gamma(0)]$ should scale as T^2. A more detailed analysis of our data (*28*) shows the expected T^2 dependence, as has been shown previously by Washburn *et al.* (*23*) and Schwartz *et al.* (*24*). The enhancement of $\Gamma(T)$ as T is increased arises from the modulation of the height of the potential barrier by thermal noise. For $T_{cr} < T < 3T_{cr}$ the escape rate is predicted to exceed the classical prediction because of the persistence of MQT into this temperature range as an additional escape process. An analysis of the data (*28*) shows reasonable agreement with predictions (*16*).

Quantized Energy Levels

In the quantum limit, we expect the energy in the potential well to be quantized, as indicated in Fig. 2d. We investigated this quantization spectroscopically by measuring the escape rate from the zero-voltage state of a high-Q junction in the presence of a microwave current. Since the microwaves induce transitions from one state to another of higher energy, and the escape rate out of the well increases when the population of higher energy states increases, we expect a resonant enhancement of the escape rate when the microwave photon energy corresponds to an energy-level spacing. In the experiment we varied the energy-level spacings by varying the bias current while keeping the microwave frequency $\Omega/2\pi$ and power P fixed. The anharmonic nature of the potential causes the energy-level spacings to decrease with increasing energy, so that each resonance corresponding to the transition between a pair of neighboring energy levels should occur at a distinct value of current.

In Fig. 6a we show the change in escape rate $[\Gamma(P) - \Gamma(0)]/\Gamma(0)$ versus bias current for an 80 by 10 μm^2 junction in the presence of 2.0 GHz microwaves. For the range of current shown there were 5 or 6 energy levels in the well, and the temperature was high enough ($k_BT/\hbar\Omega = 0.29$) for the thermal population of the lower excited states to be substantial. The damping of this junction was very low, with Q estimated to be about 75. In Fig. 6a we observe three peaks, indicating that the escape rate is resonantly enhanced at certain values of the bias current. These resonances correspond to the transitions shown in the inset. This behavior is in striking contrast to the single, asymmetric resonance observed in the classical regime.

To compare the positions of the resonances with theory we solved the Schrödinger equation numerically to find the energy levels, using values of I_0 and C obtained in the classical regime. From these calculations we obtained the energy spacings corresponding to the $0 \rightarrow 1$, $1 \rightarrow 2$, and $2 \rightarrow 3$ transitions as a function of bias current, as indicated in Fig. 6b. The intersections of these curves with the horizontal line corresponding to the microwave frequency of 2.0 GHz predict the bias currents at which the peaks should occur. The dotted curves on either side of the $0 \rightarrow 1$ curve indicate the uncertainty: the error in current arises from the uncertainty in I_0 (and hence in $I_0 - I$). A given error in I_0 shifts the three curves by the same amount. We see that the separations of the measured peaks are in excellent agreement with predictions. The absolute positions of the peaks are shifted along the current axis by about 2 parts in 3000, an error comparable with the indicated uncertainty.

A theory (*26*) for the line shape predicts that the widths of the peaks should be in the ratio 1:3:5 for the $0 \rightarrow 1$, $1 \rightarrow 2$, and $2 \rightarrow 3$ transitions. This prediction is quite well satisfied experimentally with $Q \approx 75$.

Experiments (*26*) on other junctions have shown that the position of the peak corresponding to the $0 \rightarrow 1$ transition has the correct

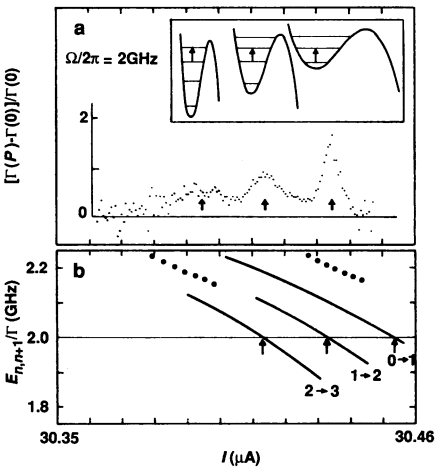

Fig. 6. (**a**) $[\Gamma(P) - \Gamma(0)]/\Gamma(0)$ versus I for an 80 by 10 μm^2 junction at 28 mK in the presence of 2.0 GHz microwaves ($k_BT/\hbar\Omega = 0.29$). Arrows indicate values of current at which the peaks of the resonances occur. Inset represents the corresponding transitions between energy levels. (**b**) Calculated energy-level spacings $E_{n,n+1}$ versus I for $I_0 = 30.572 \pm 0.017$ μA and $C = 47.0 \pm 3.0$ pF. Dotted lines indicate uncertainties in the $0 \rightarrow 1$ curve that arise from uncertainties in I_0 and C. Arrows indicate values of bias current at which resonances are predicted to occur.

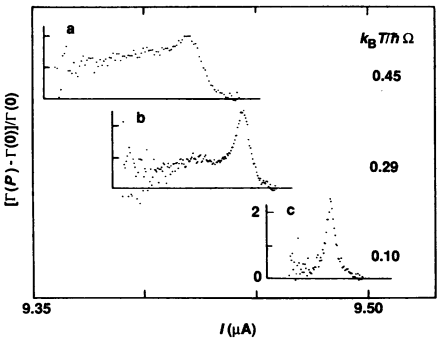

Fig. 7. $[\Gamma(P) - \Gamma(0)]/\Gamma(0)$ versus I for a 10 by 10 μm^2 junction with $I_0 \approx 9.57$ μA and $C \approx 6.35$ pF at three values of $k_BT/\hbar\Omega$. The microwave frequencies are: curve a, 4.5 GHz; curve b, 4.1 GHz; and curve c, 3.7 GHz.

dependence on microwave frequency. Resonances corresponding to the $0 \rightarrow 2$ and $1 \rightarrow 3$ transitions have also been observed. These would be strictly forbidden for a simple harmonic oscillator, but are allowed for a quadratic + cubic potential (*2*). Finally, Fig. 7 shows the evolution from quantum to classical behavior as the ratio $k_BT/\hbar\Omega$ is increased. At the lowest temperature (curve c) we observe a single, Lorentzian-shaped resonance corresponding to the $0 \rightarrow 1$ transition. At the intermediate temperature (curve b), a shoulder corresponding to the $1 \rightarrow 2$ transition appears as the thermal population of the first excited state becomes significant. At the highest temperature (curve a), the resonance is broad and asymmetric: there are several closely spaced levels in the well with substantial thermal population, and the individual transitions overlap to form a continuous response that is reminiscent of classical resonant activation.

Concluding Remarks

The experiments described above provide overwhelming evidence that the phase difference δ is a quantum variable. The measured rates of quantum tunneling of this macroscopic variable are in excellent agreement with predictions (with no adjustable parameters) both for the case where damping is negligible and for the case where the rate is reduced by a factor of about 300 by damping. These experiments show that the particle in the well is not point-like but must be described by a wave packet. The excellent agreement between experiment and theory establishes the correctness not only of the exponent of Eq. 7 but also of the prefactor, thereby vindicating the Caldeira-Legget treatment of dissipation. Furthermore, microwave spectroscopy experiments demonstrate the existence of quantized energy levels in the well, with energies in very good agreement with predictions.

Thus, our macroscopic anharmonic oscillator, namely, a Josephson junction, exhibits quantum behavior. This result shows that it is indeed possible, given enough filters and shields, to isolate a single degree of freedom in an object "big enough to get one's grubby fingers on" from all other degrees of freedom sufficiently well to observe the quantum behavior of that degree of freedom. Our system behaves very much as a "macroscopic nucleus," with quantized energy levels and a decay process (MQT) that is closely analogous to α-decay in a heavy atomic nucleus: the particle is initially in a metastable bound state and tunnels out into a continuum of states. There is a major difference, however, in that we are free to design and fabricate junctions with a wide range of parameters. Furthermore, for a given junction we can control its properties by varying I and I_0 (through an applied magnetic field). Thus, one can explore new superconducting circuits with a view both to potential device applications and to the possibility of building exotic "macroscopic nuclei with wires" that would display new quantum phenomena with no equivalents in the microscopic world.

REFERENCES AND NOTES

1. A. J. Leggett, *Prog. Theor. Phys. (Suppl.)* **69**, 80 (1980); *Contemp. Phys.* **25**, 583 (1984); *J. Phys. (Paris) Colloq.* **39**, 1264 (1980); *Essays in Theoretical Physics in Honour of Dirk Ter Haar*, W. E. Parry, Ed. (Pergamon, Oxford, 1984), p. 95.
2. See, for example, L. Schiff, *Quantum Mechanics* (McGraw-Hill, New York, ed. 3, 1968).
3. B. D. Josephson, *Phys. Lett.* **1**, 251 (1962); *Adv. Phys.* **14**, 419 (1965).
4. T. A. Fulton and L. N. Dunkleberger, *Phys. Rev. B* **9**, 4760 (1974).
5. H. A. Kramers, *Physica (Utrecht)* **7**, 284 (1940).
6. M. Büttiker, E. P. Harris, R. Landauer, *Phys. Rev. B* **28**, 1268 (1983).
7. V. I. Gol'danskii, *Dokl. Akad. Nauk SSSR* **124**, 1261 (1959); I. Affleck, *Phys. Rev. Lett.* **46**. 388 (1981).
8. Yu. M. Ivanchenko and L. A. Zil'berman, *Zh. Eksp. Teor. Fiz.* **55**, 2395 (1968) [*Sov. Phys.-JETP* **28**, 1272 (1969)].
9. A. O. Caldeira and A. J. Leggett, *Ann. Phys. (N.Y.)* **149**, 374 (1983).
10. A. J. Leggett, in *Lecture Notes, Les Houches Summer School on Chance and Matter*, J. Souletie, J. Vannimenus, R. Stora, Eds. (North-Holland, Amsterdam, 1987), p. 395; P. Hänggi, *J. Stat. Phys.* **42**, 105 (1986); H. Grabert, in *Superconducting Interference Devices and Their Applications*, H. D. Hahlbohm and H. Lübbig, Eds. (de Gruyter, Berlin, 1985), p. 289.
11. A. I. Larkin and Y. N. Ovchinnikov, *Pis'ma Zh. Eksp. Teor. Fiz.* **37**, 322 (1983) [*JETP Lett.* **37**, 382 (1983)].
12. H. Grabert, U. Weiss, P. Hänggi, *Phys. Rev. Lett.* **52**, 2193 (1984).
13. P. S. Riseborough, P. Hänggi, E. Friedkin, *Phys. Rev. A* **32**, 489 (1985).
14. W. Zwerger, *ibid.* **31**, 1745 (1985).
15. A. I. Larkin and Y. N. Ovchinnikov, *Zh. Eksp. Teor. Fiz.* **85**, 1510 (1983); *ibid.* **86**, 719 (1984) [*JETP* **58**, 876 (1983); *ibid.* **59**, 420 (1984)].
16. H. Grabert and U. Weiss, *Phys. Rev. Lett.* **53**, 1787 (1984).
17. L. D. Jackel, W. W. Webb, J. E. Lukens, S. S. Pei, *Phys. Rev. B* **9**, 115 (1974).
18. W. den Boer and R. de Bruyn Ouboter, *Physica* **98B**, 185 (1980); D. W. Bol, R. van Weelderen, R. de Bruyn Ouboter, *ibid.* **122B**, 2 (1983); D. W. Bol, J. J. F. Scheffer, W. T. Giele, R. de Bruyn Ouboter, *ibid.* **133B**, 196 (1985).
19. R. F. Voss and R. A. Webb, *Phys. Rev. Lett.* **47**, 265 (1981).
20. L. D. Jackel *et al.*, *ibid.*, p. 697.
21. R. J. Prance *et al.*, *Nature (London)* **289**, 543 (1981).
22. I. M. Dmitrenko, V. A. Khlus, G. M. Tsoi, V. I. Shnyrkov, *Fiz. Nizk. Temp.* **11**, 146 (1985) [*Sov. J. Low Temp. Phys.* **11**, 77 (1985)].
23. S. Washburn, R. A. Webb, R. F. Voss, S. M. Faris, *Phys. Rev. Lett.* **54**, 2712 (1985).
24. D. B. Schwartz, B. Sen, C. N. Archie, J. E. Lukens, *ibid.* **55**, 1547 (1985).
25. A. D. Zaiken and S. V. Panyukov, *JETP Lett.* **43**, 670 (1986). Also, J. E. Lukens, private communication.
26. J. M. Martinis, M. H. Devoret, J. Clarke, *Phys. Rev. B* **35**, 4682 (1987).
27. M. H. Devoret, J. M. Martinis, D. Esteve, J. Clarke, *Phys. Rev. Lett.* **53**, 1260 (1984); M. H. Devoret, D. Esteve, J. M. Martinis, A. Cleland, J. Clarke, *Phys. Rev. B* **36**, 58 (1987).
28. A. N. Cleland, J. M. Martinis, J. Clarke, *Phys. Rev. B*, in press.

29. We are indebted to H. Grabert, R. Landauer, S. Linkwitz, A. J. Leggett, and J. E. Lukens for helpful discussions. J.M.M. gratefully acknowledges the support of the NSF and of IBM during the course of this work. We acknowledge the use of the Microelectronics Facility in the Electronics Research Laboratory of the Electrical Engineering and Computer Science Department, University of California, Berkeley. This work was supported by the Director, Office of Energy Research, Office of Basic Energy Sciences, Materials Sciences Division of the U.S. Department of Energy under contract No. DE-AC03-76SF00098, and by the Commissariat à l'Énergie Atomique (MHD).